

Influence of grid on the extraction characteristics of different charged ions in mixed ion beams

Ao Xu(徐翱), Xiang Wan(万翔), and Pingping Gan(甘娉娉)
Citation: Chin. Phys. B, 2025, 34 (**8**): 085202. DOI: 10.1088/1674-1056/add4e0
http://cpb.iphy.ac.cn; http://iopscience.iop.org/cpb

What follows is a list of articles you may be interested in

Influence of ion species on extraction characteristics of mixed ion beams

Ao Xu(徐翱), Pingping Gan(甘娉娉), Xiang Wan(万翔), and Yuanjie Shi(石元杰)
Chin. Phys. B, 2024, 33 (**9**): 095202. DOI: 10.1088/1674-1056/ad5c3d

Global dust density in two-dimensional complex plasma

Yi-Zhen Zhao(赵逸真), Song-Fen Liu(刘松芬), Wei Kong(孔伟), and Fang Yang(杨芳)
Chin. Phys. B, 2024, 33 (**6**): 065201. DOI: 10.1088/1674-1056/ad2a76

Influence of extraction voltage on electron and ion behavior characteristics

Ao Xu(徐翱), Pingping Gan(甘娉娉), Yuanjie Shi(石元杰), and Lei Chen(陈磊)
Chin. Phys. B, 2024, 33 (**4**): 045203. DOI: 10.1088/1674-1056/ad1820

Theoretical analyses on the one-dimensional charged particle transport in a decaying plasma under an electrostatic field

Yao-Ting Wang(汪耀庭), Xin-Li Sun(孙鑫礼), Lan-Yue Luo(罗岚月), Zi-Ming Zhang(张子明), He-Ping Li(李和平), Dong-Jun Jiang(姜东君), and Ming-Sheng Zhou(周明胜)
Chin. Phys. B, 2023, 32 (**9**): 095201. DOI: 10.1088/1674-1056/ace033

Hybrid-PIC/PIC simulations on ion extraction by electric field in laser-induced plasma

Xiao-Yong Lu(卢肖勇), Cheng Yuan(袁程), Xiao-Zhang Zhang(张小章), Zhi-Zhong Zhang(张志忠)
Chin. Phys. B, 2020, 29 (**4**): 045201. DOI: 10.1088/1674-1056/ab75d8

Influence of grid on the extraction characteristics of different charged ions in mixed ion beams

Ao Xu(徐翱)†, Xiang Wan(万翔), and Pingping Gan(甘娉娉)

Institute of Electronic Engineering, China Academy of Engineering Physics, Mianyang 621999, *China*

(Received 26 February 2025; revised manuscript received 9 April 2025; accepted manuscript online 7 May 2025)

The extraction characteristics of multi-charged ions produced by ion sources are important for some useful applications. In this paper, the extraction process of Cu^{+}, Cu^{2+}, Cu^{3+}, and Cu^{4+} mixed ions is simulated by setting ideal physical parameters in a two-dimensional particle-in-cell (PIC) code, and the evolution characteristics of density and velocity distributions of different charged ions during plasma (density about 10^{15} m^{-3}) motion and extraction are presented. Besides, the effects of grid thickness and grid aperture on the motion behavior of different charged ions and the extracted ion current are analyzed. The results showed that the ion diffusion increases with the increase of the ion charge, and higher charged ions are more likely to be affected by the grid. This provides support for further understanding of the extraction characteristics of multi-charged mixed ion beams.

Keywords: ion extraction, grid, multi-charged ion, density distribution

PACS: 52.65.–y, 52.65.Rr, 29.25.–t, 29.25.Ni

DOI: 10.1088/1674-1056/add4e0 **CSTR:** 32038.14.CPB.add4e0

1. Introduction

For many plasma applications, how to extract more and higher quality ions is very important.[1–3] Therefore, many researchers have studied the principle and influencing factors of ion extraction, and given the effects of ion source,[4,5] electrode configuration,[6–10] plasma density,[11] electron temperature,[12] ion species,[13,14] ion thermal velocity,[15] extraction voltage,[16] space charge effect,[17–19] background pressure,[20–22] plasma sheath,[23–25] etc. on ion extraction characteristics. In addition, as some application systems need to use grid to shield the electric field or improve the ion distribution, some researchers have also studied the influence of grid on ion extraction. For example, Alekseev obtained the effect of grid on ion energy distribution by experiments, and pointed out that the effect is obviously dependent on ion mass.[26] Lu analyzed the influence of the decelerator grid on the optical performance, and found that it can greatly affect the downstream charge-exchange ions.[27] Chen simulated the transport processes of plasmas in grid systems of krypton ion thrusters, and obtained that the screen grid transparency increases with the acceleration voltage and decreases with the beam current.[28] Sun studied the influence of different grid structures on the plasma characteristics in the discharge chamber, and gives recommendations for grid structures suitable for ion thrusters with different sizes.[29] Laya presented a numerical optimization of the theoretical screen grid aperture diameter and total aperture count for maximum screen grid ion transparency in ion thrusters.[30] Rovang obtained the influence of grid structure on ion extraction capability in the two-grid accelerator systems by a large number of experiments.[31] In addition, grid materials[32] and grid erosion[33,34] have also been studied. However, these studies have not considered the influence of grid on the extraction of multi-charged ions, especially, the extraction characteristics of different charged ions are different. At present, a small number of studies on the extraction of multi-charged ions only focus on the design of electrode structures and the characteristics of the extraction current.[35–37] Therefore, in order to analyze the influence of grid on the extraction characteristics of different charged ions, the extraction process of Cu^{+}, Cu^{2+}, Cu^{3+}, and Cu^{4+} mixed ions is simulated by setting ideal physical parameters in a particle-in-cell (PIC) code. The evolution characteristics of density and velocity distributions of different charged ions during extraction are presented, and the influences of grid thickness and grid aperture on the motion characteristics of different charged ions are analyzed. This provides support for further understanding of the extraction characteristics of multi-charged mixed ion beams.

2. Simulation model

In practical application system, the proportion of different charged ions produced by ion sources is different. In order to more clearly analyze the distribution characteristics and extraction capabilities of different charged ions in mixed ion beams, this paper utilizes the two-dimensional (2D) PIC method to establish an ideal simulation model (It is assumed that the fluxes of different charged ions injected into the plasma chamber are the same) for the extraction process of

†Corresponding author. E-mail: xuao@caep.cn

© 2025 Chinese Physical Society and IOP Publishing Ltd. All rights, including for text and data mining, AI training, and similar technologies, are reserved.

mixed ion beams. The schematic diagram is shown in Fig. 1. The model consists of a plasma chamber, grids, and an extraction electrode. They are made of metal. The calculated area is 10 mm×(10.9+d) mm. d represents the grid thickness and the wall thickness at the top of the plasma chamber. The inner length and height of the plasma chamber are 9.8 mm and 5 mm, respectively. The gird length and grid aperture are 0.1 mm and L, respectively. The distance between the plasma chamber and the extraction electrode is 5.9 mm, and the plasma injection area is 3-mm long. The voltage of the extraction electrode is −1000 V, while the plasma chamber and the grid are grounded. Both sides of the area without electrodes are set as Neumann boundary condition.

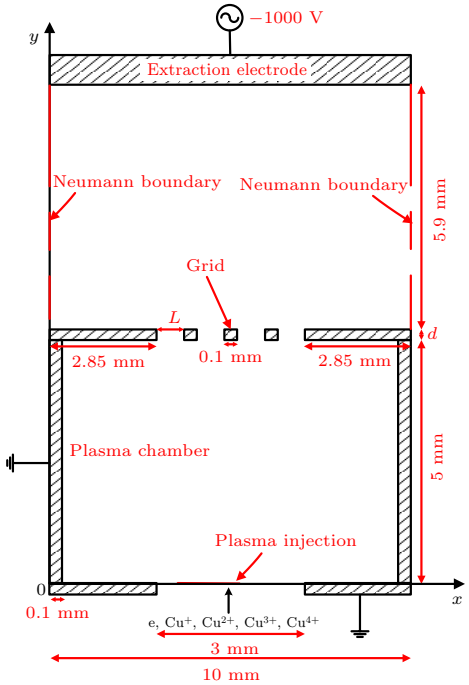


Fig. 1. Schematic diagram of simulation area.

The simulated particles are electrons, Cu^{+}, Cu^{2+}, Cu^{3+}, and Cu^{4+}, and the secondary electron emission resulting from particle bombardment on the wall is not taken into account. All particles bombarded on the surface of the metallic wall are absorbed and the surface charge accumulation effect is not considered.

In the plasma injection area, the flux of the electrons is set as 6×10^{21} $m^{-2}\cdot s^{-1}$ with a temperature of 5 eV and velocity of 1×10^{5} m/s, and the fluxes of Cu^{+}, Cu^{2+}, Cu^{3+}, Cu^{4+} are all set as 1×10^{19} $m^{-2}\cdot s^{-1}$ with a temperature of 0.1 eV and velocity of 1×10^{4} m/s. Moreover, the initial velocity distributions of these particles are all set as Maxwell distribution.

In PIC simulation, it is generally required that the grid length (spatial step) is less than the Debye length, and the time step is less than the reciprocal of the plasma frequency and satisfies the Courant–Friedrichs–Lewy (CFL) condition.[38,39] Therefore, in our simulation, the time step of the simulation is 10^{-12} s, and the grid length step is 0.025 mm.

3. Typical simulation results

On the basis of the simulation model in the previous chapter, we set the grid thickness to $d = 0.3$ mm and the grid aperture to $L = 1$ mm. The density distributions of different particles at different times are simulated. The results are shown in Fig. 2.

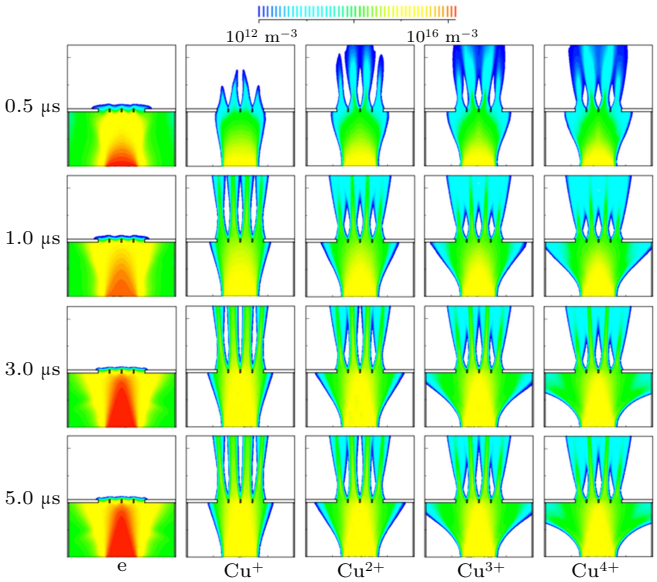


Fig. 2. Density distributions of different particles at different time.

As it can be seen from Fig. 2 that the results have converged and stabilized at 5 μs, the simulation results at 5 μs are discussed in the following sections. It can also be found that as the ions move from the injection region to the grid, the higher charge of the ion, the more significant its diffusion.

The potential distribution in the middle region (x = 5.5 mm, y = 0 mm–11.2 mm) is shown in Fig. 3. It can be found that the potential in the plasma chamber is very small. Therefore, it can be deduced that in the plasma motion process, the ion with higher charge diffusing more should be due to the space charge force which has a greater effect on the ion with higher charge.

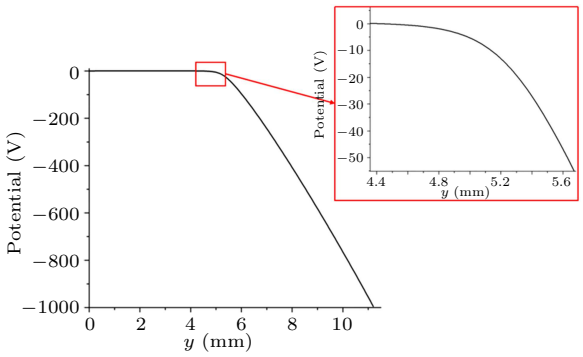


Fig. 3. Potential distribution in the middle region.

In addition, from Fig. 2, we can also found that the Cu^{+} ion beam is divided into four parts by the number of "holes" in the grid after it is extracted from the grid. In the process

of moving towards the extraction electrode, the parts on both sides are compressed first, and then diverged, while the two parts in the middle move almost linearly. The reason for this phenomenon is that the x-direction electric field component in the middle region of the grid is small, while that on the two sides of the grid is large, as shown in Fig. 4 (the x-direction component of the electric field near the grid ($x = 0$ mm–10 mm, $y = 5.5$ mm)). Therefore, the ion beams on the two sides are more obviously changed by the x-direction electric field force. It is worth noting that the electric field between the plasma chamber and the extraction electrode is mainly in the y-direction. However, although the grids are grounded, the electric field can still "penetrate" into the plasma chamber through the holes, resulting in the direction of the electric field passing through the hole being partially deflected by the grid potential (grounding), thus forming the x-direction electric field component. Moreover, the middle region of the grids is full of plasma, which has a "shielding" effect on the electric field, so that the x-direction electric field component on both sides of the grids is large, while that in the middle is small.

In addition, after the Cu^{4+} ion beam is extracted, its four parts are first compressed and then diverged. The parts on the two sides are more obvious than the two parts in the middle. This indicates that the higher charged ion beam is more easily confined by the electric field force, and even over-focused.

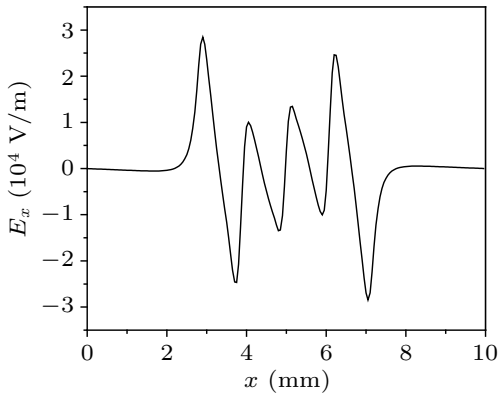


Fig. 4. The x-direction component of the electric field near the grid.

The different ion density and velocity distributions at the extraction electrode ($x = 0$ mm–10 mm, $y = 11.2$ mm) are shown in Figs. 5 and 6, respectively. It can be found that higher charged ions have a higher ion velocity at the extraction electrode, and the ion density is lower, but the ion density distribution is more uniform. This is because higher charged ions diffuse more significant in the plasma chamber, resulting in fewer of these ions being extracted. In addition, higher charged ions are more likely to be accelerated by the extracted electric field, thus increasing the velocities. Besides, compared with the injected ion current (The 2D simulation cannot directly obtain the ion current, it is assumed that the simulation results within 1 mm perpendicular to the simulation area are the same, and thus the ion current is calculated), the proportion of higher charged ions in the extracted ion current is lower, as shown in Fig. 7.

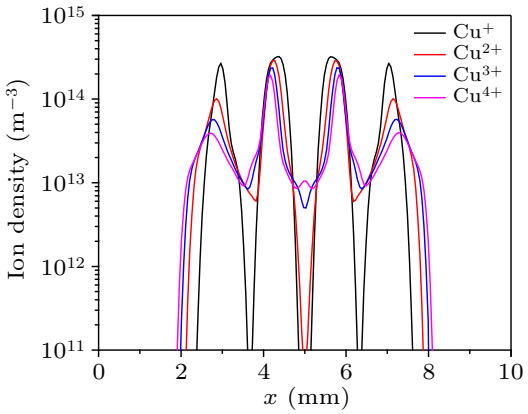


Fig. 5. Density distribution of different ions at the extraction electrode.

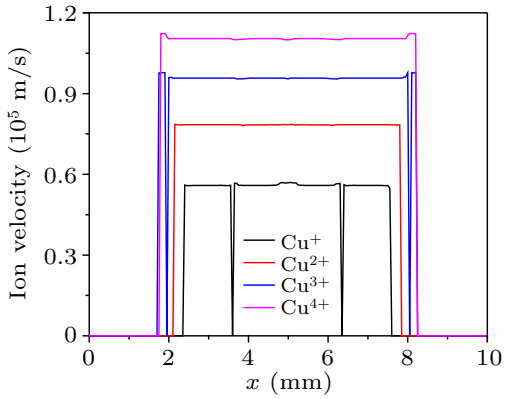


Fig. 6. Velocity distribution of different ions at the extraction electrode.

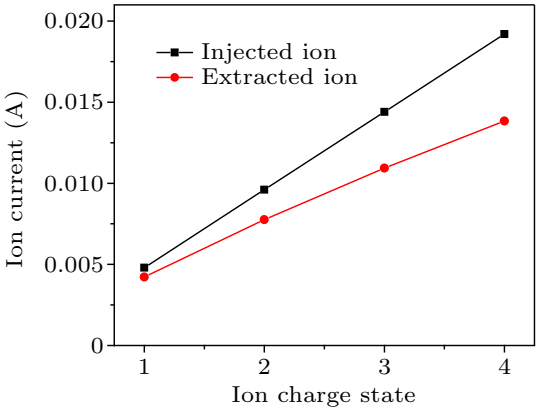


Fig. 7. Ion current of different ions.

4. Simulation results of different grid thickness

Based on the above simulation model, other settings remain unchanged, only the grid thickness (d) is set to 0.1 mm, 0.3 mm, and 0.5 mm, respectively. The influence of the grid thickness on the particle density distribution is simulated, as shown in Fig. 8.

It can be seen from Fig. 8 that the diffusion of ions in the plasma chamber increases slightly as the grid thickness increases. From the potential distribution inside the grid ($x =$

0 mm–10 mm, $y = 4.9$ mm), as shown in Fig. 9, it can be found that with the increase of the gird thickness, the amplitude of the negative potential inside the grid decreases, which means that the electric field "penetrating" into the plasma chamber from the grid hole also decreases. And this also reduces the force of the electric field "penetrating" into the plasma chamber on electrons and ions, increases the expansion time of the plasma, and leads to more diffusion of ions in the plasma chamber.

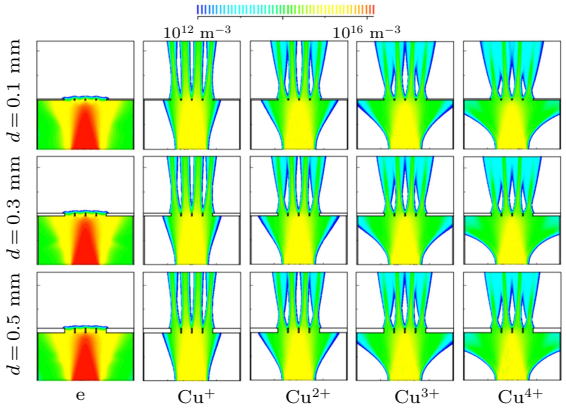


Fig. 8. Influence of grid thickness on particle density distribution.

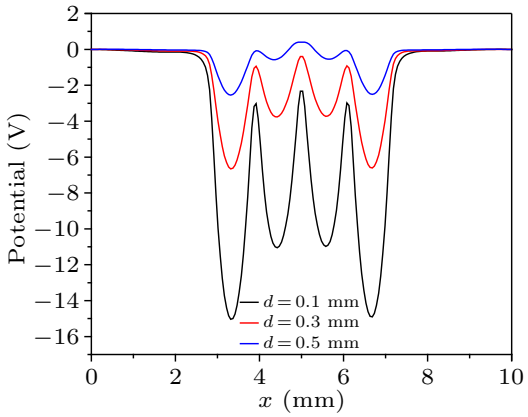


Fig. 9. Potential distribution inside the grid.

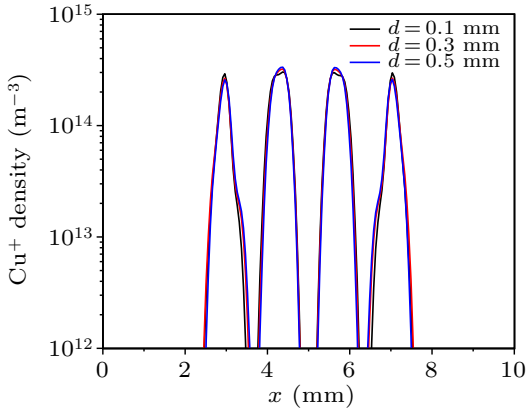


Fig. 10. Cu^{+} density distribution at the extraction electrode.

Comparing the density distributions of Cu^{+}, Cu^{2+}, Cu^{3+}, and Cu^{4+} at the extraction electrode ($x = 0$ mm–10 mm, $y = 11$ mm, 11.2 mm, and 11.4 mm, respectively), as shown in Figs. 10–13, it can be seen that the grid thickness has a more obvious effect on the higher charged ions, and the density distribution of the higher charged ions is more concentrated. This may be related to the fact that with the increase of

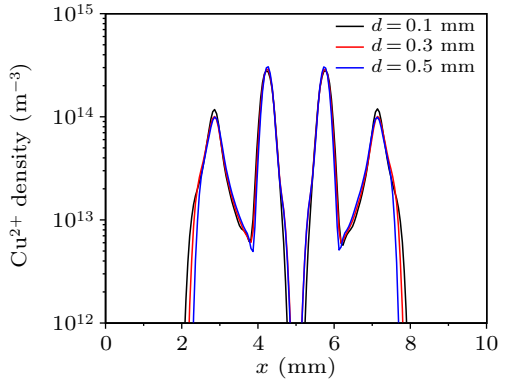


Fig. 11. Cu^{2+} density distribution at the extraction electrode.

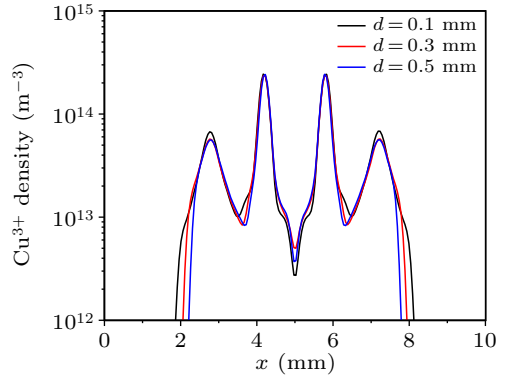


Fig. 12. Cu^{3+} density distribution at the extraction electrode.

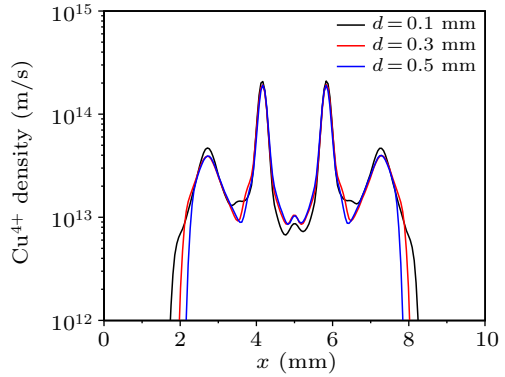


Fig. 13. Cu^{4+} density distribution at the extraction electrode.

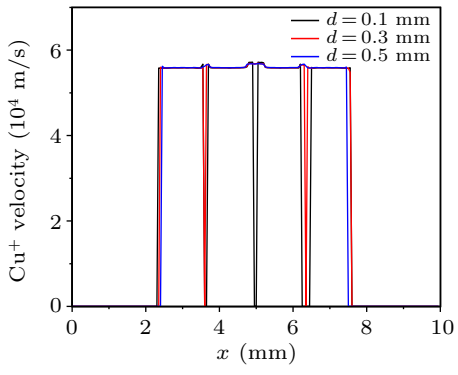


Fig. 14. Cu^{+} velocity distribution at the extraction electrode.

grid thickness and the higher charge of the ion, the less number of ions can be extracted from the plasma chamber. However, the grid thickness has no significant effect on the velocities of different charged ions, as shown in Figs. 14–17.

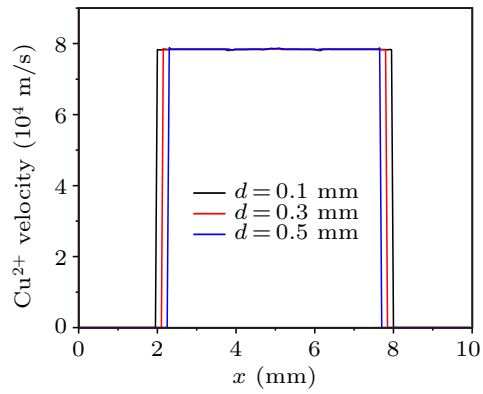


Fig. 15. Cu^{2+} velocity distribution at the extraction electrode.

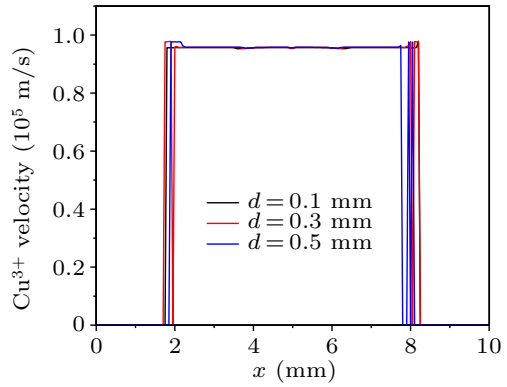


Fig. 16. Cu^{3+} velocity distribution at the extraction electrode.

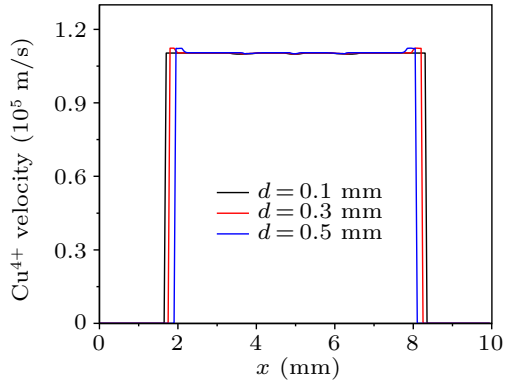


Fig. 17. Cu^{4+} velocity distribution at the extraction electrode.

The ion currents of different charged ions at the extraction electrode under the conditions of different grid thicknesses are shown in Fig. 18. It can be seen that with the increase of the grid thickness and the charge of the ion, the ion current reduced more. On the one hand, it should be noted that the decrease of the extracted ion current may be due to the ion diffusion in the plasma chamber leading to the loss of recombination with the wall. On the other hand, the loss may be caused by the ion collisions to the grid. The increase of the grid thickness will not only make the ion diffuse more significant in the plasma chamber, but also increase the possible "contact area" between the grid and the ions. Therefore, it is necessary to analyze which factor has a greater impact. Comparing the ion current loss caused by ions bombardment to the plasma chamber body (The definition here is that the ion current loss caused by ions bombardment to the wall of the plasma chamber except the grid, i.e., I_{wall}.) with the ion current loss caused by the grid (I_{grid}), as shown in Figs. 19 and 20, it can be obtained that the ion current loss caused by ion bombardment to plasma chamber body (except the grid, I_{wall}) is relatively greater. In addition, the grid thickness has little effect on the extracted ion current of lower charged ions, but has great effect on the extracted ion current of higher charged ions. Moreover, this effect of "greater effect on the extraction of higher charged ions" is more obvious in the ion current loss

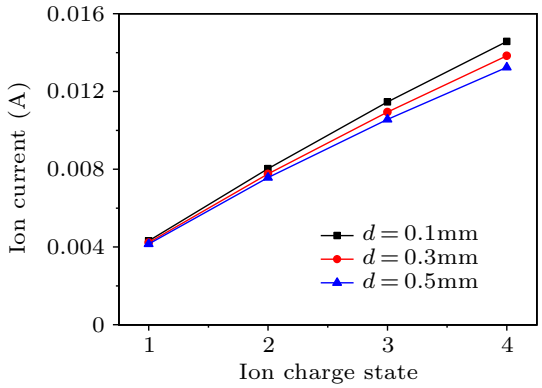


Fig. 18. Influence of grid thickness on extracted ion current of different charged ions.

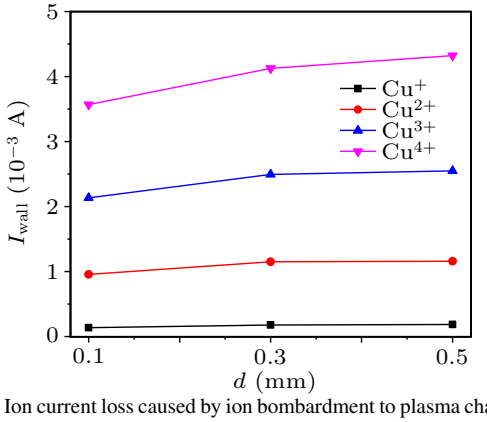


Fig. 19. Ion current loss caused by ion bombardment to plasma chamber (except the grid) under different grid thicknesses.

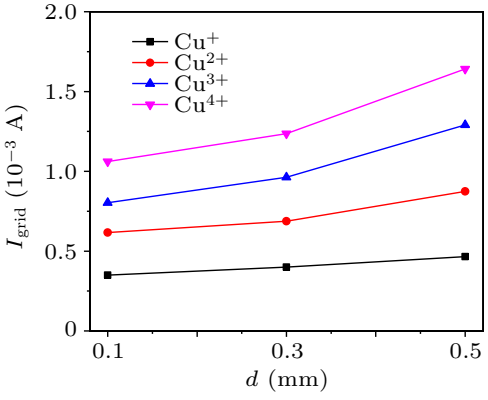


Fig. 20. Ion current loss caused by grid under different grid thicknesses.

caused by the grid. This indicates that many ions will bombard on not only the lower surface of the grid, but also the sides of the grid when the ions move through the grid. In this process, the grid at ground potential has a stronger "attraction" to positive higher charged ions.

Our simulation model does not consider the secondary electron emission generated by the ion bombardment to the wall. According to the simulation results, the energy of ions in the plasma chamber will not exceed hundreds of electron volts, so the secondary electrons emission yield produced by these ion bombardment walls is also less than 0.1.[40] Moreover, the maximum ion density near the plasma chamber is only 10^{15} m^{-3}, which will lead to fewer secondary electrons generated by the ion bombardment to the plasma chamber, and these electrons will leave the wall quickly. Therefore, the influence of these secondary electrons on the simulation results can be ignored.

5. Simulation results of different grid aperture

Still based on the above simulation model, keeping other settings unchanged, but the grid thickness is set to 0.3 mm, and the grid aperture (L) is set to 2.1 mm, 1 mm, and $\sim$ 0.63 mm, respectively. The influence of the grid aperture on the particle density distribution is simulated and shown in Fig. 21.

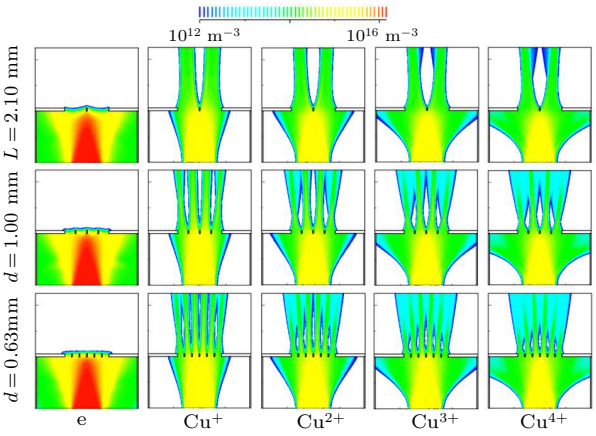


Fig. 21. Influence of grid aperture on particle density distribution.

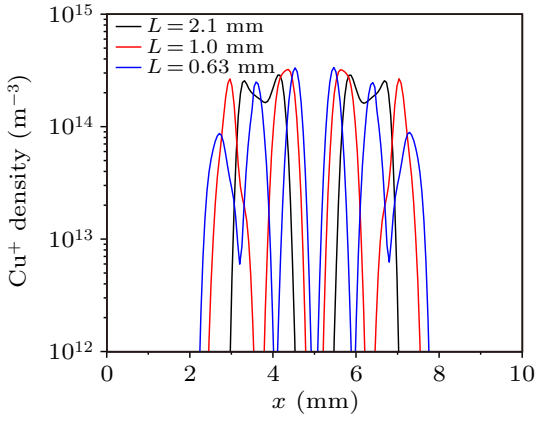


Fig. 22. Cu^{+} density distribution at the extraction electrode.

The density distributions of the different ions at the extraction electrode ($x = 0$ mm–10 mm, $y = 11.2$ mm) are shown in Figs. 22–25.

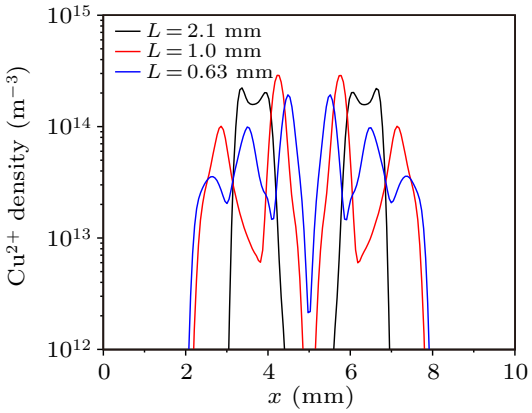


Fig. 23. Cu^{2+} density distribution at the extraction electrode.

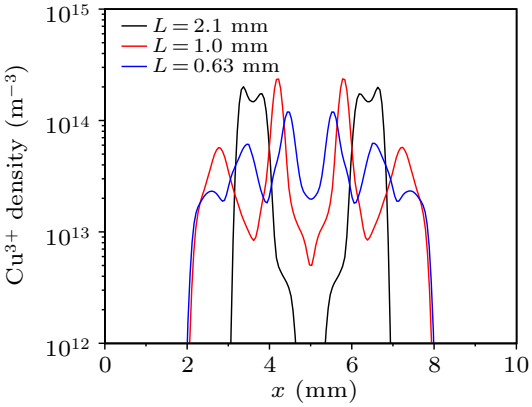


Fig. 24. Cu^{3+} density distribution at the extraction electrode.

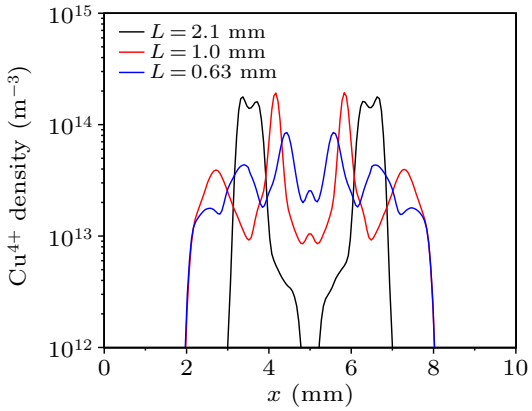


Fig. 25. Cu^{4+} density distribution at the extraction electrode.

As it can be seen from Figs. 21–25, the movement of the higher charged ions is more obviously affected by the electric field force, same as the results in the previous section. In addition, with the decrease of the grid aperture (that is, the grid "holes" are more but smaller), the density distributions of different charged ions at the extraction electrode are all relatively more uniform. However, the grid aperture has no significant effect on the ion velocity at the extraction electrode, as shown in Figs. 26–29.

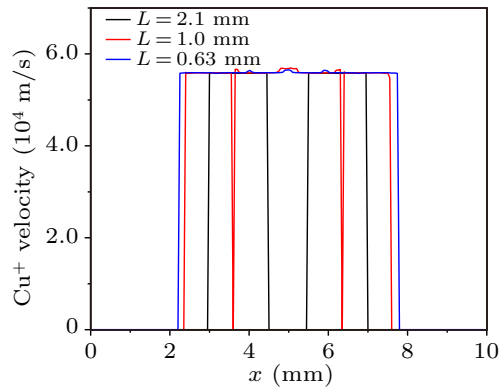


Fig. 26. Cu^+ velocity distribution at the extraction electrode.

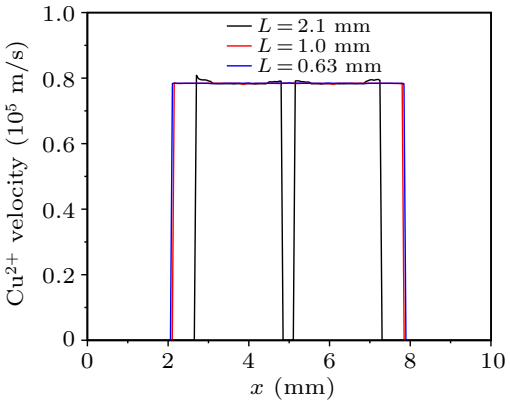


Fig. 27. Cu^{2+} velocity distribution at the extraction electrode.

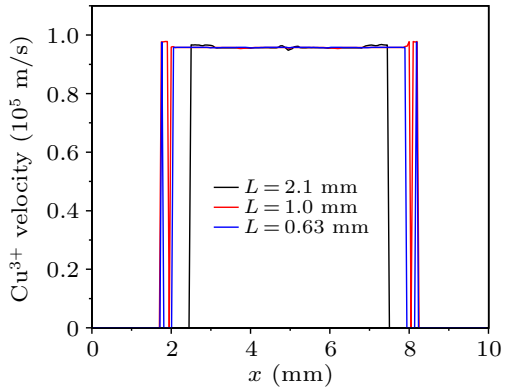


Fig. 28. Cu^{3+} velocity distribution at the extraction electrode.

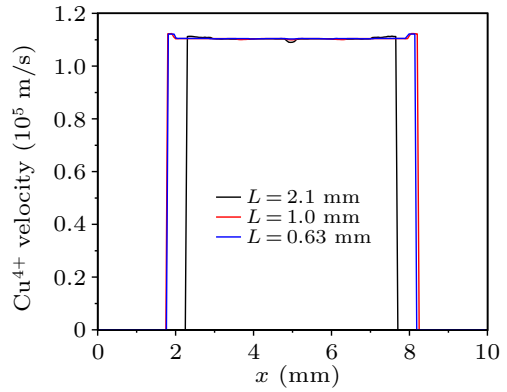


Fig. 29. Cu^{4+} velocity distribution at the extraction electrode.

Further analysis of the influence of the grid aperture on the ion current of different charged ions at the extraction electrode, as shown in Fig. 30, it can be obtained that with the decrease of the grid aperture, and the higher charge of the ion, the more of the ion current loss. Through the ion current changes of different charged ions on the inside of the grid ($x = 2.85$ mm–7.15 mm, $y = 4.99$ mm), as shown in Fig. 31, it is shown that with the decrease of the grid aperture, the higher charged ions will slightly lose more ion current in the plasma chamber. Therefore, it can be inferred that the main reason for the variation of the extracted ion current caused by the grid aperture is that the area of the grid "blocking" the movement of ions outward from the plasma chamber increases. Besides, higher charged ions are more likely to be "attracted" by the grid and lost.

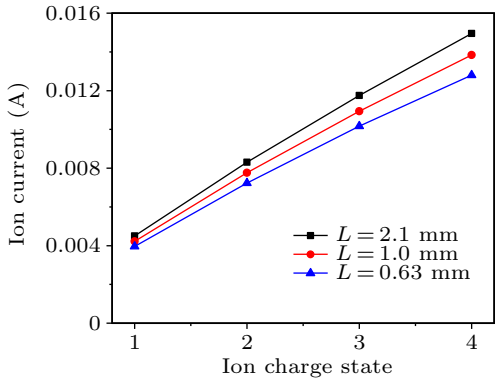


Fig. 30. Influence of grid aperture on extracted ion current of different charged ions.

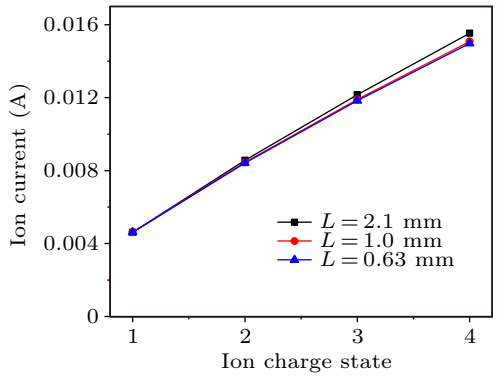


Fig. 31. Ion current of different charged ions on the inside of the grid.

6. Conclusions

In this paper, the influence of grid on the extraction process of different charged ions (plasma density about 10^{-15} m^{-3}) from a plasma chamber is analyzed by 2D PIC simulations at −1000-V extraction voltage, and the following conclusions can be drawn.

(i) In a plasma chamber with a small electric field that "penetrates" the grid, as the plasma continues to move, the higher the charge of an ion, the more pronounced its diffusion. This is because the more charge an ion has, the more it is affected by the space charge force. Similarly, in the process of ions moving from the grid to the extraction electrode, the

higher charged ions are also more likely to be affected by the electric field force, resulting in changes in their motion characteristic.

(ii) With the increase of grid thickness and ion charge, the more of the ion current loss. The main reason for this is that the increase of the grid thickness makes more ions bombard and lose on the side of the grid when they pass through the grid. In addition, the increase of the grid thickness reduces the electric field "penetrating" into the plasma chamber, so that the diffusion of higher charged ions in the plasma chamber is more significant, which is also the reason for the loss of the extracted current.

(iii) With the decrease of the grid aperture, the density distribution of ions on the extraction electrode becomes more uniform, and its effect on the extraction ion current is mainly reflected in the increase of the area of "blocking" ions passing through the grid, thereby decreasing the ion current. As the higher charge ions are more affected by the electric field force, the extracted ion current loss will be relatively more.

Acknowledgements

Project supported by the Presidential Foundation of China Academy of Engineering Physics (Grant No. YZJJZQ2022016), and the National Natural Science Foundation of China (Grant No. 52207177).

References

[1] Aston G, and Wibur P J 1981 *J. Appl. Phys.* **52** 2614
[2] Whealton J H, Jaeger E F and Whitson J C 1977 *Rev. Sci. Instrum.* **48** 829
[3] Wang Y T, Sun X L, Luo L Y, Zhang Z M, Li H P, Jiang D J and Zhou M S 2023 *Chin. Phys. B* **32** 095201
[4] Nakano M, Yamamoto N, I Funaki and Ohkawa Y 2018 *Tran. JSASS Aerospace Tech. Japan* **16** 98
[5] Spadtke P 2018 *Rev. Sci. Instrum.* **89** 081101
[6] Keller R 1990 *Nuclear Instruments and Methods in Physics Research A: Accelerators, Detectors, Associated Equipment* **298** 247
[7] Soliman B A, Abdelrahman M M, Helal A G and Abdelsalam F W 2011 *Chin. Phys. C* **35** 83
[8] Singh P and Maiti N 2024 *Phys. Scr.* **99** 025609
[9] Lee M, Kim J Y, Kim Y, Hwang Y S and Chung K J 2023 *IEEE Trans. Plasma Sci.* **51** 1404
[10] Svotina V V and Khartov S A 2024 *Acta Astronautica* **215** 653
[11] Dorf M A, Sidorov A V, Zorin V G, Bohanov A F, Vodopyanov A V, Izotov I V, Razin S V and Skalyga V A 2007 *J. Appl. Phys.* **102** 054504
[12] Chen J, Fu T Z, Guo H, Li H P, Jiang D J and Zhou M S 2019 *Plasma Sci. Technol.* **21** 045402
[13] Hatamil M M and Kourakis I 2022 *Sci. Rep.* **12** 6905
[14] Xu A, Gan P P, Wan X and Shi Y J 2024 *Chin. Phys. B* **33** 095202
[15] Li H L and Sun A B 2021 *Comput. Phys. Commun.* **259** 107629
[16] Xu A, Gan P P, Shi Y J and Chen L 2024 *Chin. Phys. B* **33** 045203
[17] Kosonen S T, Kalvas T, Tarvainen O and Toivanen V 2022 *J. Phys.: Conf. Ser.* **2244** 012079
[18] Lafleur T and Aanesland A 2014 *Phys. Plasmas* **21** 123506
[19] Shen Z, Sun L T, Jia Z H, Fang X, Qian C and Zhao H W 2022 *J. Phys.: Conf. Ser.* **2244** 012090
[20] Wei H L, Cao J Y, Rao J, Lei G J, Jiang S F, Liu H, Yu L M, Xie W M, Li M, Yang X F, Zou G Q, Lu D L and Duan X R 2012 *Rev. Sci. Instrum.* **83** 023302
[21] Toivanen V, Steczkiewicz O, Tarvainen O, Ropponen T, Arje J and Koivisto H 2010 *Nuclear Instruments and Methods in Physics Research B: Beam Interactions with Materials and Atoms* **268** 1508
[22] Xu A, Wan X, Gan P P and Shi Y J 2025 *IEEE Trans. Plasma Sci.* **53** 252
[23] Baalrud S D, Scheiner B, Yee B T, Hopkins M M and Barnat E 2020 *Plasma Sour. Sci. Technol.* **29** 053001
[24] Beving L P, Hopkins M M and Baalrud S D 2022 *Plasma Sour. Sci. Technol.* **31** 084009
[25] Benedikt J, Kersten H and Piel A 2021 *Plasma Sources Science and Technology* **30** 033001
[26] Alekseev N, Balabaev A, Khrisanov I, Kulevoy T, Losev A, Satov Y, Shumshurov A and Vasilyev A 2020 *Rev. Sci. Instrum.* **91** 033304
[27] Lu C, Zhao Y D, Wan J, Chu Y C, Zheng L and Cao Y 2019 *International Journal of Aerospace Engineering* **2019** 8916303
[28] Chen M L, Sun A B, Chen C and Xia G Q 2018 *Chinese Journal of Aeronautics* **31** 719
[29] Sun M M, Long J F, Guo W L, Liu C and Zhao Y 2023 *Plasma Sci. Technol.* **25** 015509
[30] Laya N and Xu K G 2022 *AIAA SCITECH* 2022 *Forum*, January 3–7, 2022, San Diego, CA & Virtual, USA
[31] Rovang D C and Wilbur P J 1985 *Journal of Propulsion and Power* **1** 172
[32] Zhang S Q, Li A J, Zheng Y Q and Zhang D S 2019 *Appl. Math. Mech.* (English edition) **40** 1589
[33] Lu C, Wang Y L, Geng H, Xia G Q and Li J 2022 *IEEE Trans. Plasma Sci.* **50** 50
[34] Rahaman S E, Singh A K, Shukla S K and Barik R K 2017 *IEEE Trans. Plasma Sci.* **45** 2974
[35] Kirtsev D V, Akimova A A, Galchuk A V, Klopenkov R M, Mudrolyubov V G and Osina Y K 2023 *Phys. Particles Nucl. Lett.* **20** 796
[36] Kato Y, Sugiyama S and Ishii S 2002 *Rev. Sci. Instrum.* **73** 601
[37] Anderson O A and Logan B G 1998 *Rev. Sci. Instrum.* **69** 1106
[38] Tskhakaya D, Matyash K, Schneider R and Taccogna F 2007 *Contributions to Plasma Physics* **47** 563
[39] Fierro A, Moore C H, Yee B and Hopkins M 2018 *Plasma Sour. Sci. Technol.* **27** 105008
[40] Lieberman M A and Lichtenberg A J 2005 *Principles of Plasma Discharges and Materials Processing*, 2nd edn. (John Wiley & Sons, Inc.: New Jersey) p. 302